Title	Rapid, versatile, and reliable metrology for multi-layer transition metal dichalcogenide thin films using atomic force microscopy to investigate surface grain distributions
Authors	Tonon, Alessandro;Gupta, Aashi;Di Russo, Enrico;Sheehan, Brendan;Metaxa, Pavlina;Arifutzzaman, A.;Connolly, J.;Lin, Jun;Povey, Ian M.;Sgarbossa, Francesco;De Salvador, Davide;Napolitani, Enrico;Duffy, Ray
Publication date	2025-09-23
Original Citation	Tonon, A., Gupta, A., Di Russo, E., Sheehan, B., Metaxa, P., Arifutzzaman, A., Connolly, J., Lin, J., Povey, I., Sgarbossa, F., De Salvador, D., Napolitani, E. and Duffy, R. (2025) 'Rapid, versatile, and reliable metrology for multi-layer transition metal dichalcogenide thin films using atomic force microscopy to investigate surface grain distributions', Applied Physics Letters, 127(12), 123102 (8pp). https://doi.org/10.1063/5.0276152
Type of publication	Article (peer-reviewed)
Link to publisher's version	10.1063/5.0276152
Rights	© 2025, AIP Publishing. This article may be downloaded for personal use only. Any other use requires prior permission of the author and AIP Publishing. The following article appeared in Tonon, A., Gupta, A., Di Russo, E., Sheehan, B., Metaxa, P., Arifutzzaman, A., Connolly, J., Lin, J., Povey, I., Sgarbossa, F., De Salvador, D., Napolitani, E. and Duffy, R. (2025) 'Rapid, versatile, and reliable metrology for multi-layer transition metal dichalcogenide thin films using atomic force microscopy to investigate surface grain distributions', Applied Physics Letters, 127(12), 123102 (8pp). https://doi.org/10.1063/5.0276152 and may be found at https://pubs-aip-org.ucc.idm.oclc.org/aip/apl/article/127/12/123102/3364340/Rapid-versatile-and-reliable-metrology-for-multi.
Download date	2026-09-19 18:14:38

Rapid, versatile, and reliable metrology for multi-layer transition metal dichalcogenide thin-films using Atomic Force Microscopy to investigate surface grain distributions

A. Tonon[1,*,†], A. Gupta[2,†], E. Di Russo[1,3,4], B. Sheehan[2], P. Metaxa[2], A. Arifutzzaman[2], J. Connolly[2], J. Lin[2], I. Povey[2], F. Sgarbossa[1,3], D. De Salvador[1,3], E. Napolitani[1,3], R. Duffy[2]

[1] Università Degli Studi di Padova, Dipartimento di Fisica e Astronomia, via Marzolo 8, Padova, 35131, Italy.

[2] Tyndall National Institute, University College Cork, Lee Maltings, Cork T12 R5CP, Ireland.

[3] Istituto Nazionale di Fisica Nucleare, Laboratori Nazionali di Legnaro, Viale dell'Università 2, 35020, Legnaro, Italy

[4] CNR-ISMN, Via Gobetti 101, 40129, Bologna, Italy

[†]) Both authors contributed equally to this work.
[*]) Corresponding author: alessandro.tonon.7@phd.unipd.it

ABSTRACT

Molybdenum disulfide (MoS_2) has garnered significant attention among 2D materials, demonstrating great potential for electronics and optoelectronics. Although numerous growth techniques have been explored, a definitive solution for large-area film fabrication remains elusive. Moreover, comparing thin-films obtained through different techniques is not straightforward. Particularly, analyzing grain size across samples is challenging, making it difficult to clearly correlate growth conditions with the resulting crystal structure. In this letter, we developed an approach based on atomic force microscopy (AFM) morphology measurements to analyze nanograins in large-area thin-films obtained through relevant growth techniques such as chemical vapor deposition (CVD) and sputter deposition followed by pulsed laser annealing (PLA). To address the challenges in comparing thin-films grown by different methods, we propose a robust approach based on statistical grain analysis. By combining well-established investigation tools, such as AFM, with advanced watershed-segmentation algorithms, we demonstrate a reliable method for identifying grains and

grain boundaries. This approach allows for a robust and quantitative comparison of film morphology across different growth conditions, providing a crucial benchmark for evaluating and differentiating various growth methods.

Our approach represents a simple and fast grain size study which can be used as a first analysis tool before moving to more complex characterization, such as transmission electron microscopy (TEM), while analyzing large areas of interest and thus obtaining statistical information on sample grains. Furthermore, this technique can be combined with complementary characterization methods to rapidly determine the role of grain size and boundaries in influencing other film properties relevant for electrical applications.

Transition metal dichalcogenide (TMD) thin-film synthesis processes and strategies for large areas have progressed rapidly over the past few years[1,2], and it is vital metrology keeps pace with advancements in this field. Rapid, versatile, and reliable feedback through material characterization can greatly facilitate the selection of synthesis routines and techniques.

For electron device applications, few-layer (FL) thin-films are often preferred due to their higher current density output. However, due to the polycrystalline nature of atomic layer deposition (ALD) [3,4], chemical vapor deposition (CVD) [5,6], or sputtered films [7,8], grain sizes and boundary defects [9] can negatively affect the semiconductor properties [10]. As a result, the capability to measure such grain sizes and locate boundary defects becomes crucial. The characterization of a FL thin-film system is quite challenging in comparison to mono-layer (ML) case, due to potentially overlapping grains at different depths within the FL material.

It is the aim of this work to demonstrate how atomic force microscopy (AFM) can provide efficient and effective analysis to provide rapid turnaround feedback suitable for the material synthesis and electron device communities. It should bear in mind that AFM, like other microscopy and spectroscopy methods, should not be a stand-alone solution, but rather it should be used in combination with other techniques such as Raman, scanning electron microscopy (SEM), X-ray photoelectron spectroscopy (XPS), and transmission electron microscopy (TEM), for the determination of thin-film crystallinity, stoichiometry, surface morphology, and cross-sectional structure. By applying appropriate metrology tools to a material system, one can build up a robust data set to draw an informed conclusion [11]. In this work, we will be focusing on the specific role that AFM can play in this procedure.

At this stage it is worth noting that a number of advanced techniques has been applied to characterize TMD thin-films and analyze crystal structure and grain sizes. Much work was done on monolayers (ML), often with incomplete surface coverage, as that is the cleanest system to map grain sizes, however statistical data analysis is still sparse. Fan et al. used a vapor HF based etching

technique to visualize grain boundaries in MoS_2 by SEM and AFM, as the acid preferentially etched the underlying substrate [12]. Karvonen et al. applied multi-phonon microscopy to study ML MoS_2 and compare it to other techniques such as Raman and photoluminescence [13]. The spectroscopy visualization performed by Park et al. gave an insight into ML and bi-layer MoS_2 also deposited by CVD [14]. In the work by Zhang et al. it was observed that the grain boundaries in WS_2 films preferentially oxidize, thus making them appear more readily in SEM [15]. Preferential oxidation along edges has also been seen in exfoliated flakes previously [16]. Visualization of grains in TMD films was also performed by scanning transmission electron microscopy (STEM), applied to MoS_2 synthesized from metallic Mo films [17]. Lastly, a statistical data analysis was applied to AFM data by Gong et al., however in the context of film roughness, rather than grain sizes [18].

AFM was applied to TMD thin-films in both hardware and software considerations. Key hardware requirements for studying ML TMD thin-films are AFM scanning modes and high-resolution tips. The use of ultra-fine (2 nm) probe tips can simplify map analysis, such as the Bruker ScanAsystAir-HPI used for part of this work. However, it is the aim of this work to demonstrate how a robust grains analysis can be obtained independently of the specific AFM setup. Software issues relate to the post-processing routines applied to the raw data collected on the AFM tool. A well thought out post-processing routine is crucial for a statistical analysis of the thin-film grains sizes.

Furthermore, the type of feedback required by the end-user may depend on the application or discipline involved. Device engineers may require a close inspection of grain sizes and boundary defects to locate the areas in the thin-film where the grains are large, in order to fabricate a prototype device in that region, thus limiting the impact of grain boundary defects on device performance. Equally, material chemists involved in developing optimized TMD thin-film deposition processes, may choose to examine the statistics of the synthesized thin-film when comparing new methods, precursors, or processing parameters. MoS_2 thin-film samples were synthesized using either CVD or sputter deposition followed by pulsed laser annealing (PLA). Sputtered samples were deposited using

magnetron RF sputtering (13.56 MHz) with a molybdenum disulfide target (99.95% purity) onto 90 nm SiO_2-on-Si substrates. The deposition was carried out in a high-purity Ar_2 gas atmosphere at a pressure of 5×10^{-3} mBar with an electrical power of 40 W applied to the cathode. The initial sputter deposition produced amorphous material, which was subsequently subjected to PLA using a 22 ns KrF 248 nm excimer pulsed laser to induce crystallization of MoS_2. CVD samples (~10 nm) were grown between 250 and 550 ºC using CVD in a 300 mm atomic layer deposition reactor utilizing $Mo(CO)_6$ and 1% H_2S (99.999%) in Ar as the precursors, on 85 nm SiO_2-on-Si substrates. The CVD films were several layers thick, and polycrystalline in nature.

AFM was performed for morphological characterization of sample surface. Surface morphology maps were collected using a Bruker Dimension Icon AFM working in PeakForce Tapping mode in combination with ScanAsystAir and ScanAsystAir-HPI tips (nominal tip radius of curvature of 2 nm). Similar to traditional tapping, in PeakForce Tapping mode the probe periodically taps the sample while the interaction force is measured through cantilever deflection, and the peak force is kept constant through a feedback loop. This setup is designed to achieve high-resolution measurements of small structures, thanks to no cantilever tuning and low and controllable imaging forces: expected variation in lateral feature dimensions is <1 nm. Tip convolution broadening is limited thanks to small radius of curvature, and thermal drift is minimized by prior thermal stabilization (15 minutes) and by confirming image fidelity with AFM trace/retrace consistency. Additionally, the self-optimizing algorithm ScanAsyst was used during PeakForce scanning allowing for fast and automated adjustment of scan parameters (setpoint, feedback response, scan rate). Additional measurements were performed using a Nanosurf FlexAFM microscope operated in semi-contact mode using BudgetSensors ElectriMulti75-G probes (nominal tip radius of curvature of 25 nm).

Software analysis on the acquired AFM map was performed using the free and Open-Source software Gwyddion [19]. This software was used for data correction, statistical characterization and grain marking.AFM maps were collected for CVD and PLA samples. Two representative images are

reported in Figure 1a and 1b. The surface morphology of each sample displays a nanometric grain structure. Note, when studying a FL thin-film, the AFM data reflects the grain structure and morphology of the top layer of the polycrystalline film. In our analysis, we do not assume the grains detected at the surface extend through the entire film depth.

In the CVD sample, typical triangular grain domains are observed, as expected for MoS_2 thin films grown on Si/SiO_2 substrates. These overlapping grains cover the whole sample surface. The morphology map reveals a clear contrast between the center and the edges of each triangular grain, likely due to oxidation of grain boundaries, which causes fractures and elevated areas compared to the inner part of each flake [20].

In contrast, PLA samples do not exhibit triangular shapes to help grains identification. This difference is attributed to the Mo-rich composition of annealed films [7,21]. While dodecahedral domains are theoretically expected in sulfur deficient films, experimental studies showed that circular domains are favored when the Mo/S ratio is the limiting growth factor [22]. Furthermore, sulfur vacancies promote oxidation during ultrafast laser treatments [23], increasing surface roughness as shown in Figure 1. The distinct surface morphologies between the two synthesis methods must be carefully considered in map analysis, especially in how grain centers are identified. Noise in AFM maps can interfere with accurate grain identification, requiring effective noise suppression. Additionally, a reliable analysis method must account for MoS_2 film discontinuities, such as out-of-plane grains in CVD samples and voids between grains in PLA samples.

For these reasons, a watershed-algorithm [24] was chosen for map analysis. The segmentation results for selected AFM maps are shown in Figure 1, where the starting AFM maps are reported together with the intermediate and final steps of the segmentation. The chosen watershed-algorithm is composed of two steps, grain localization and complete image segmentation.

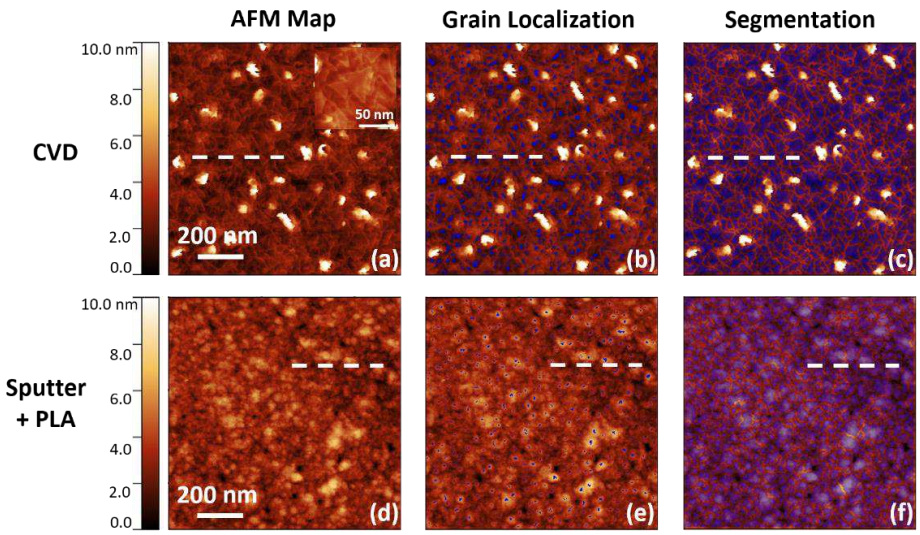

Fig. 1: Representative AFM maps for CVD (a-c) and PLA (d-f) MoS_2 films. The three columns represent the different stages of grain analysis: initial AFM map (a, d), identification of grain position (b, e), and segmentation of the map (c, f) to identify grain boundaries. For each map, a profile (white dashed line) is extracted and reported in Fig.2. Inset of (a): zoom in showing triangular MoS_2 grains with lateral size between 20 and 50 nm.

To clarify the two-steps process, two profiles were extracted from AFM maps, reported in Figure 1, one for the CVD sample and one for the PLA sample and reported in Figure 2. The final profile is divided into two regions: grains (including the initial grain locations marked in blue) and grain boundaries. The watershed algorithm, widely applied to image segmentation and grain analysis [24,25], for both isolated and overlapping grain structures Additionally, noise sensitivity can be adjusted to suit AFM map acquisition in thin-film materials. Grain analysis follows two stages as detailed in [25]:

1. The watershed algorithm simulates "water drops" of a fixed volume applied sequentially at each surface point, following the steepest descent toward a local minimum. This procedure works directly for CVD samples where oxidized grain boundaries are higher than the inner

region of the grain. Alternatively, the 'gravity force' can be inverted resulting in the local maxima of the AFM maps to be identified, which is preferable for grains protruding from the surface, as in PLA samples. When a drop reaches a local minimum, it partially fills its volume, as shown in Figure 1b and e. This process is repeated for a fixed number of steps to identify local minima and to merge closely positioned ones and to progressive fill their volume. Smaller basins are removed by comparison with a fixed area threshold (obtained by projecting the basin volume) to minimize noise artefacts. The identified grains are marked and saved for the second step. In Figure 2, blue areas correspond to initial grain seeds, found at local minima in CVD samples (Figure 2a) and local maxima in PLA samples (Figure 2b). Not all the local minima/maxima are marked due to noise thresholding.

2. Water drops of fixed size are positioned again at each map point, following the steepest descent toward local minima. This iterative process continues for a fixed number of steps, further filling the features. Drops reaching a marked grain or a closest neighboring position merge into the grain, increasing its volume. If a drop encounters two different closest neighboring grains, it identifies a grain boundary. Subsequent drops reaching a marked grain boundary merge with it, increasing its volume similarly to grains. As reported in Figure 2, this results in a mask applied to the sample surface, segmenting the map into grains and grain boundaries.

The segmentation procedure was tuned for each sample according to its morphological properties as demonstrated in Figure 2: CVD triangular grains were identified starting from local minima while PLA samples grains were marked starting from local maxima.

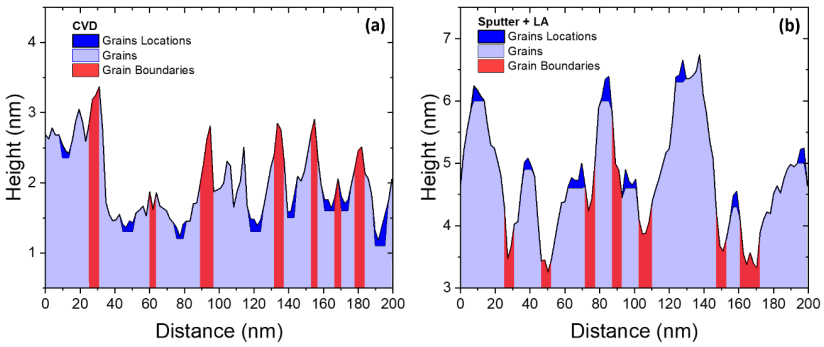

Fig. 2: Extracted profiles from AFM maps reported in Fig. 1. After the segmentation process, grains and grains boundaries are identified from local minima in CVD samples (a) and local maxima in PLA samples (b).

The watershed-algorithm requires to be tuned to obtain reproducible and consistent results [26–28]. Parameters were optimized by considering the AFM setup and the resulting grain size distributions, reported in Figure 3. The number of repetitions of water drops falling at each position and their volume have a strong impact on the number and size of identified grains. The necessity to introduce a noise threshold requires a sufficient filling of local minima/maxima in the localization step, otherwise only a minority of grains is identified [29]. Insufficient filling (Figure 3a and 3e) results in an increased grain size average and lower grains count, as shown in Figure 3d and 3h. Similarly, an overflow incorrectly merges distinct neighboring grains (Figure 3c and 3g), resulting in fewer grains with increased average size. Increasing drops volume or repetition leads to higher grains counts and a decrease average size, until the merging of adjacent grains becomes dominant, producing fewer and larger grains. By choosing parameters within an optimal range between these two endpoints, the method remains robust, converging to similar distributions with only minor differences. The insets of Figure 3d and 3h report average grain size and dispersion versus step number at fixed drop volume. The most stable conditions occur at ~75 steps for both CVD and PLM samples with 0.25% drop

volume. Below this threshold, grains are underfilled and cut during identification, while segmentation causes size overestimation by extending boundaries. Beyond 75 steps, average size increases slightly but dispersion rises due to long tails originating from incorrectly merged grains. Both sample types show similar trends, even if with differences depending on growth conditions: this could be explained by MoS_2 films having similar thickness, roughness, and estimated grain size.

Systematic fine-tuning can be performed by analyzing the obtained grain size distribution: non-optimal parameters combination results in a large number of very small grains that produce a bimodal distribution with a secondary peak near zero, distorting the actual tail. Minimizing such artefacts allows the method to converge to stable distributions. The noise-cutting threshold should be comparable to the scan pixel size and the nominal AFM tip radius of curvature, which is especially critical for separated grains. Depending on the AFM setup, this threshold may need to be increased to reduce noise artefacts. Analysis of the grain size distribution allows to systematically tune the noise threshold: if small grains are underrepresented due to a truncated distribution, it should be reduced. Conversely, an excess of grains near zero suggests increasing the threshold to eliminate noise artifacts. The threshold was set at 9 px^2 (~6 nm), producing a distinct secondary peak around 1.5 nm, clearly originating from image noise, since such features cannot be resolved with 2 nm AFM tip. Regarding the second step, parameters selection controls the segmentation of features like out-of-plane grains or film discontinuities. Limiting the volume filled for each identified grain avoids the inclusion of these regions: optimal parameters were identified at 2.0% drop size and 300 steps.

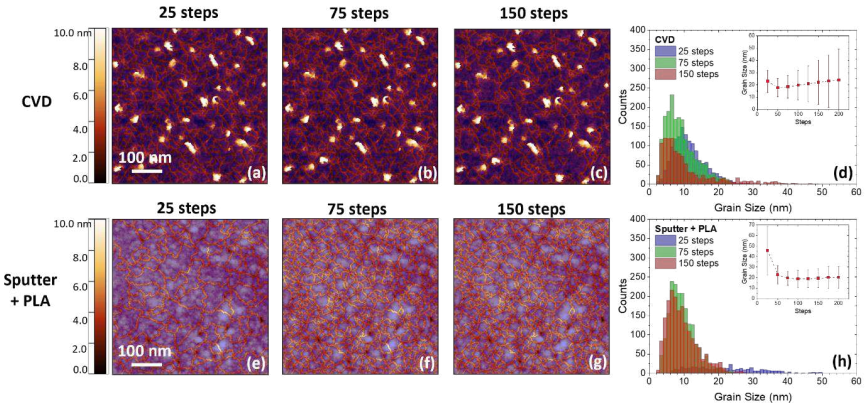

Fig. 3: AFM maps for CVD (a-c) and PLA (e-g) MoS_2 films with segmentations obtained with different number of steps during identification stage. The corresponding distributions are presented separately for CVD (d) and PLA (h) films. Insets: average grain size and dispersion trend versus number of steps at fixed drop volume for CVD (d) and PLA (h) films.

Grains statistical analysis was applied to study film behaviors under different growth conditions. For the two discussed synthesis techniques, CVD and sputtering followed by PLA, temperature and laser energy density (ED) play a crucial role in determining the crystalline structure. In CVD samples, temperature controls material quality and out-of-plane growth, whereas in PLA film, ED is the key factor controlling the degree of crystallinity [7,21]. As reported in Figure 4, growth conditions impacted on grain size distributions. In CVD samples, the average grain size decreases from 26 to 20 nm, increasing growth temperature while decreasing the grain size dispersion; estimated through the root mean square (RMS). At 550 °C, the distribution is more peaked around the average value, with a higher grain counts due to fewer out-of-plain grains, which are always excluded from segmentation. Conversely, PLA samples exhibit an opposite trend. Increasing ED to 125 mJ/cm^2 shifts grains distribution toward larger size, correlating with film degradation and isolated coalescence formation [7,21]. Samples processed with 75 and 100 mJ/cm^2 show similar average values and RMS, but 100 mJ/cm^2 samples present a smoother distribution, as shown in Figure 4, aligning

with previous findings of improved uniformity at this ED level. The analysis on PLA samples was repeated with an alternative AFM instrument with a larger tip radius, producing comparable results. A slight increase in average grain size was observed, likely due to the larger tip, but overall, the method demonstrated consistency across different instruments.

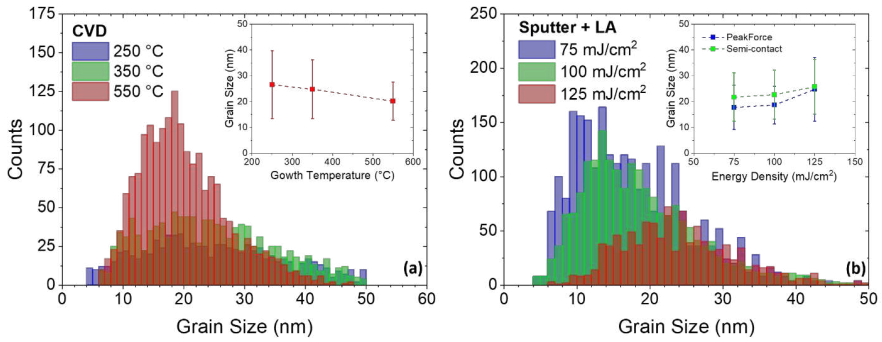

Fig. 4: Grain size distributions for CVD (a) and PLA (b) samples. Average values and standard deviation for each distribution are reported in the corresponding insets. For PLA, a comparison between AFM measurements performed with different instruments is reported.

AFM maps were collected for identical samples using two setups, differing in scanning mode and tip radii. Despite these differences, trends in grain size distribution remain consistent, allowing reliable comparison between samples measured under the same conditions. Detailed observations across modes and tip convolution are reported in the supplementary material.

This work demonstrated the possibility of using AFM scanning as a quick and reliable tool for surface grains analysis in TMDs thin-films. The proposed analysis using watershed-algorithm for grain identification proved to be effective at image segmentation, with enough flexibility to adapt to specific sample characteristics such as the presence of oxidized grain boundaries and out-of-plane growth. The proposed methodology was applied to multi-layer films allowing to achieve consistent results on nanostructured surfaces. Statistical analysis of grain population is a fundamental tool to

understand and correlate sample properties measured through different growth techniques and conditions. Thus, the proposed approach for the identification of surface grain size and boundaries could significantly enhance the optimization of film growth and device fabrication and characterization, even though additional characterization with complementary techniques is required to investigate vertical extension of grains. In both CVD and PLA samples, the impact of different growth conditions was studied showing an evolution of grain populations coherent with previous reports about material properties. Furthermore, the analysis was applied to maps obtained through different AFM instruments and configurations, highlighting differences that reflects setup characteristics, such the type of used AFM tips, but still producing reliable and reproducible results.

SUPPLEMENTARY MATERIAL

AFM maps were collected for identical samples using two setups at the University of Padova, Italy, and Tyndall National Institute, Ireland. The setups differ in scanning modes, Semi-contact (tapping) and Peak-Force, and in tip radii. Semi-contact mode with larger tip convolution shifts grain size distribution toward larger grains, but trend remains consistent between the two setups. Discussion and analysis are reported in supplementary material. This consistency enables reliable comparison between samples measured under the same conditions.

ACKNOWLEDGMENTS

This work was supported by the European Commission through project ASCENT+: Access to European Infrastructure for Nanoelectronics, funded under H2020, grant 871130, and the project "Network 4 Energy Sustainable Transition—NEST", Spoke 1., Project code PE0000021, funded under the National Recovery and Resilience Plan (NRRP), Mission 4, Component 2, Investment 1.3— Call for tender No. 1561 of 11.10.2022 of Ministero dell'Universita` e della Ricerca (MUR); funded by the European Union—NextGenerationEU, the Italian Ministry of University and Research (MUR) by the Departments of Excellence grant 2023-2027 "Quantum Frontiers", and by the

University of Padova through the project UNIPD-ISR 2017 "SENSITISE". This publication has also emanated from research supported in part by a grant from Research Ireland under Grant number 21/FFP-A/9897. L. Bacci and N. Argiolas (University of Padova) are acknowledged for their technical assistance.

AUTHOR DECLARATION

Conflicts of interest

The authors have no conflicts to disclose.

Author contributions

A. Tonon: Conceptualization, Formal analysis, Methodology, Investigation, Visualization, Writing – original draft. **A. Gupta:** Formal analysis, Investigation, Methodology, Visualization. **E. Di Russo:** Supervision, Writing – review & editing. **B. Sheehan:** Investigation, Methodology. **P. Metaxa:** Methodology. **A. Arifutzzaman:** Methodology. **J. Connolly:** Resources, Investigation. **J. Lin:** Resources, Investigation. **I. Povey:** Resources, Investigation. **F. Sgarbossa:** Methodology. **D. De Salvador:** Methodology, Funding acquisition**. E. Napolitani:** Conceptualization, Supervision, Funding acquisition, Writing – review & editing. **R. Duffy:** Conceptualization, Methodology, Supervision, Funding acquisition, Writing – review & editing, Project administration.

Data Availability

The data that support the findings of this study are available from the corresponding author upon reasonable request.

REFERENCES

[1] O. Samy, S. Zeng, M.D. Birowosuto, and A. El Moutaouakil, "A review on MoS2 properties, synthesis, sensing applications and challenges," Crystals (Basel), (2021).

[2] Z. Ye, C. Tan, X. Huang, Y. Ouyang, L. Yang, Z. Wang, and M. Dong, "Emerging MoS2 Wafer-Scale Technique for Integrated Circuits," Nanomicro Lett **15**(1), (2023).

[3] M. Mattinen, F. Gity, E. Coleman, J.F.A. Vonk, M.A. Verheijen, R. Duffy, W.M.M. Kessels, and A.A. Bol, "Atomic Layer Deposition of Large-Area Polycrystalline Transition Metal Dichalcogenides from 100 °c through Control of Plasma Chemistry," Chemistry of Materials **34**(16), 7280–7292 (2022).

[4] Y. Huang, L. Liu, W. Zhao, and Y. Chen, "Preparation and characterization of molybdenum disulfide films obtained by one-step atomic layer deposition method," Thin Solid Films **624**, 101–105 (2017).

[5] J. Lin, S. Monaghan, N. Sakhuja, F. Gity, R.K. Jha, E.M. Coleman, J. Connolly, C.P. Cullen, L.A. Walsh, T. Mannarino, M. Schmidt, B. Sheehan, G.S. Duesberg, N. McEvoy, N. Bhat, P.K. Hurley, I.M. Povey, and S. Bhattacharjee, "Large-area growth of MoS2at temperatures compatible with integrating back-end-of-line functionality," 2d Mater **8**(2), (2021).

[6] F. Chen, Q. Lv, Y. Xia, S. Mao, and Y. Li, "Controllable Synthesis of Large-Scale Monolayer MoS2Dendritic Flakes with Serrated Edges and Their Multimodal Microscopy and AFM Characterizations," Journal of Physical Chemistry C **126**(31), 13449–13457 (2022).

[7] E. Di Russo, A. Tonon, A. Mischianti, F. Sgarbossa, E. Coleman, F. Gity, L. Panarella, B. Sheehan, V.A. Lebedev, D. De Salvador, R. Duffy, and E. Napolitani, "Synthesis of Large-Area Crystalline MoS2by Sputter Deposition and Pulsed Laser Annealing," ACS Appl Electron Mater **5**(5), 2862–2875 (2023).

[8] G. Jayaram, N. Doraiswamy, L.D. Marks, and M.R. Hilton, *Ultrahigh-Vacuum High-Resolution Transmission Electron Microscopy of Sputter-Deposited M0S2 Thin Films* (1994).

[9] W. Zhou, X. Zou, S. Najmaei, Z. Liu, Y. Shi, J. Kong, J. Lou, P.M. Ajayan, B.I. Yakobson, and J.C. Idrobo, "Intrinsic structural defects in monolayer molybdenum disulfide," Nano Lett **13**(6), 2615–2622 (2013).

[10] C.J. Dorow, T. Schram, Q. Smets, K.P. O'Brien, K. Maxey, C.C. Lin, L. Panarella, B. Kaczer, N. Arefin, A. Roy, R. Jordan, A. Oni, A. Penumatcha, C.H. Naylor, M. Kavrik, D. Cott, B. Groven, V. Afanasiev, P. Morin, I. Asselberghs, C.J. Lockhart de la Rosa, G. Sankar Kar, M. Metz, and U. Avci, "Exploring manufacturability of novel 2D channel materials: 300 mm wafer-scale 2D NMOS & PMOS using MoS2, WS2, & WSe2," (2023 International Electron Devices Meeting (IEDM)), (2023).

[11] M. Georgieva, N. Petkov, and R. Duffy, "3D to 2D perspectives - Traditional and new doping and metrology challenges at the nanoscale," Mater Sci Semicond Process **163**, (2023).

[12] X. Fan, R. Siris, O. Hartwig, G.S. Duesberg, and F. Niklaus, "Rapid and Large-Area Visualization of Grain Boundaries in MoS2on SiO2Using Vapor Hydrofluoric Acid," ACS Appl Mater Interfaces **12**(30), 34049–34057 (2020).

[13] L. Karvonen, A. Säynätjoki, M.J. Huttunen, A. Autere, B. Amirsolaimani, S. Li, R.A. Norwood, N. Peyghambarian, H. Lipsanen, G. Eda, K. Kieu, and Z. Sun, "Rapid visualization of grain boundaries in monolayer MoS2 by multiphoton microscopy," Nat Commun **8**, (2017).

[14] S. Park, M.S. Kim, H. Kim, J. Lee, G.H. Han, J. Jung, and J. Kim, "Spectroscopic Visualization of Grain Boundaries of Monolayer Molybdenum Disulfide by Stacking Bilayers," ACS Nano **9**(11), 11042–11048 (2015).

[15] Y. Zhang, Y. Zhang, Q. Ji, J. Ju, H. Yuan, J. Shi, T. Gao, D. Ma, M. Liu, Y. Chen, X. Song, H.Y. Hwang, Y. Cui, and Z. Liu, "Controlled growth of high-quality monolayer WS2 layers on sapphire and imaging its grain boundary," ACS Nano **7**(10), 8963–8971 (2013).

[16] G. Mirabelli, C. McGeough, M. Schmidt, E.K. McCarthy, S. Monaghan, I.M. Povey, M. McCarthy, F. Gity, R. Nagle, G. Hughes, A. Cafolla, P.K. Hurley, and R. Duffy, "Air sensitivity of MoS2, MoSe2, MoTe2, HfS2, and HfSe2," J Appl Phys **120**(12), (2016).

[17] C.J. Perini, M.J. Muller, B.K. Wagner, and E.M. Vogel, "Low-temperature, plasma assisted, cyclic synthesis of MoS2," Journal of Vacuum Science & Technology B, Nanotechnology and Microelectronics: Materials, Processing, Measurement, and Phenomena **36**(3), (2018).

[18] C. Gong, J. Xiao, L. Zhu, M. Qi, and S. Ma, "Crystal structure and tribological properties of molybdenum disulfide films prepared by magnetron sputtering technology," Current Applied Physics **19**(12), 1318–1324 (2019).

[19] D. Nečas, and P. Klapetek, "Gwyddion: An open-source software for SPM data analysis," Central European Journal of Physics **10**(1), 181–188 (2012).

[20] Y. Zhang, Y. Zhang, Q. Ji, J. Ju, H. Yuan, J. Shi, T. Gao, D. Ma, M. Liu, Y. Chen, X. Song, H.Y. Hwang, Y. Cui, and Z. Liu, "Controlled growth of high-quality monolayer WS2 layers on sapphire and imaging its grain boundary," ACS Nano **7**(10), 8963–8971 (2013).

[21] A. Tonon, E. Di Russo, F. Sgarbossa, L. Bacci, N. Argiolas, C. Scian, Y.P. Ivanov, G. Divitini, B. Sheehan, D. De Salvador, A. Gasparotto, V. Morandi, R. Duffy, and E. Napolitani, "Laser induced crystallization of sputtered MoS2 thin films," Mater Sci Semicond Process **164**, (2023).

[22] J. Sitek, J. Plocharski, I. Pasternak, A.P. Gertych, C. Mcaleese, B.R. Conran, M. Zdrojek, and W. Strupinski, "Substrate-Induced Variances in Morphological and Structural Properties of MoS2Grown by Chemical Vapor Deposition on Epitaxial Graphene and SiO2," ACS Appl Mater Interfaces **12**(40), 45101–45110 (2020).

[23] A. V. Emelianov, M. Pettersson, and I.I. Bobrinetskiy, "Ultrafast Laser Processing of 2D Materials: Novel Routes to Advanced Devices," Advanced Materials **36**(30), (2024).

[24] L. Vincent, and P. Soille, "Watersheds in digital spaces: an efficient algorithm based on immersion simulations," IEEE Trans Pattern Anal Mach Intell **13(06)**, 583–598 (1991).

[25] P. Klapetek, I. Ohlídal, D. Franta, A. Montaigne-Ramil, A. Bonanni, D. Stifter, and H. Sitter, *Atomic Force Microscopy Characterization of ZnTe Epitaxial Films* (2003).

[26] N. Zerrouki, A. Zouina Ait-Djafer, F. Harrou, S. Lafane, S. Abdelli-Messaci, and Y. Sun, "Image-driven machine learning for automatic characterization of grain size and distribution in smart vanadium dioxide thin films," Measurement (Lond) **233**, (2024).

[27] J. Barraud, "The use of watershed segmentation and GIS software for textural analysis of thin sections," Journal of Volcanology and Geothermal Research **154**(1–2), 17–33 (2006).

[28] I.S. Ezad, J.F. Einsle, D.P. Dobson, S.A. Hunt, A.R. Thomson, and J.P. Brodholt, "Improving grain size analysis using computer vision techniques and implications for grain growth kinetics," American Mineralogist **107**(2), 262–273 (2022).

[29] G. Xiang, T. Rong, G. Li, and L. Yao, "Grain Size Characterization of Ceramic Matrix Composites," Int J Mach Learn Comput **11**(4), 317–322 (2021).